Synthesis of Titanium-Containing Block, Random, End-Functionalized, and Junction-Functionalized Polymers via Ruthenium-Catalyzed Living Radical Polymerization and Direct Observatio...

ARTICLE *in* MACROMOLECULES · JANUARY 2014

Impact Factor: 5.8 · DOI: 10.1021/ma402332g

5 AUTHORS, INCLUDING:

Kotaro Satoh
Nagoya University
111 PUBLICATIONS **1,881** CITATIONS
SEE PROFILE

Hiroshi Jinnai
Tohoku University
234 PUBLICATIONS **4,234** CITATIONS
SEE PROFILE

Macromolecules

Article

pubs.acs.org/Macromolecules

Synthesis of Titanium-Containing Block, Random, End-Functionalized, and Junction-Functionalized Polymers via Ruthenium-Catalyzed Living Radical Polymerization and Direct Observation of Titanium Domains by Electron Microscopy

Yasutaka Tsujimoto,[†] Kotaro Satoh,*[,†] Hidekazu Sugimori,[‡,#] Hiroshi Jinnai,*[,§,∥] and Masami Kamigaito*[,†]

[†]Department of Applied Chemistry, Graduate School of Engineering, Nagoya University, Furo-cho, Chikusa-ku, Nagoya 464-8603, Japan

[‡]Department of Macromolecular Science and Engineering, Graduate School of Science and Engineering, Kyoto Institute of Technology, Matsugasaki, Sakyo-ku, Kyoto 606-8585, Japan

[#]KRI, Inc., 6-19-9 Torishima, Konohana-ku, Osaka 554-0051, Japan

[§]Institute for Materials Chemistry and Engineering (IMCE), Kyushu University, 744 Motooka, Nishi-ku, Fukuoka 819-0395, Japan

[∥]Japan Science and Technology Agency, ERATO, Takahara Soft Interfaces Project, CE80, Kyushu University, 744 Motooka, Nishi-ku, Fukuoka 819-0395, Japan

Supporting Information

ABSTRACT: A series of well-defined titanium-containing random, diblock, and triblock copolymers were prepared by ruthenium-catalyzed living radical polymerization of glycidyl methacrylate followed by amination of the epoxy group with diethanolamine and titanium complex loading, which was achieved by reacting the resulting triethanolamine pendent group with $CpTiCl_3$ or Cp^*TiCl_3 (Cp: cyclopentadienyl; Cp*: pentamethylcyclopentadienyl). The titanium-containing unit obtained by this procedure possessed a discrete atrane structure, which contributed to the formation of soluble well-defined polymers without cross-linking via uncontrolled intermolecular multisite ligation to the titanium center. In addition, the Cp* derivatives were highly stable to moisture. The same strategy was used successfully to construct well-defined titanium end-functionalized polymers, and an epoxy-functionalized initiator was used in the ruthenium-catalyzed living radical polymerization of methyl methacrylate, followed by postreactions with diethanolamine and Cp^*TiCl_3. The titanium-containing block copolymers were analyzed by electron energy loss spectroscopy, transmission electron microscopy, and transmission electron microtomography to directly observe titanium-containing phases in the microphase-separated block copolymers.

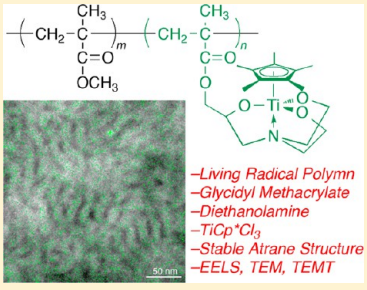

INTRODUCTION

The well-defined conjugation of organic macromolecules or polymers with metals can lead to special functions, as observed in optoelectronic materials, magnetic materials, supported catalysts, and metalloenzymes.[1−6] One of the most efficient synthetic methods for the preparation of metal-containing macromolecules is the controlled/living polymerization of metal-containing monomers or precursor monomers with functional groups, into which metal parts can be subsequently introduced via controlled ligation. However, metal or ligand parts in the monomers often interact or react with the propagating species, especially in ionic polymerizations, which induces side reactions and results in the production of uncontrolled polymers. In addition, the loading of metal species into the functionalized groups of monomer units often leads to the aggregation or cross-linking of polymer chains via uncontrolled intermolecular multisite coordination to the metal and the formation of insoluble products. Therefore, the judicious design of polymerization systems, monomers, and metals and/or ligating sites is crucial for the construction of well-defined metal-containing polymers.

Recent years have seen significant developments in controlled/living radical polymerizations. In such polymerizations, various vinyl monomers can be polymerized in a controlled fashion to obtain a wide variety of well-defined polymers with controlled molecular weights and unique polymer structures, such as end-functionalized polymers, blocks, grafts, and stars.[7−17] Because of the presence of a neutral radical propagating species, monomers containing polar functional monomers can be directly polymerized in a controlled manner without the use of protective groups; however, the polymerization system must be judiciously designed based on the monomer type. As evidenced by the tremendous number of recent papers on this subject,

Received: November 11, 2013
Revised: January 3, 2014
Published: January 17, 2014

Scheme 1. Synthesis of Various Titanium-Containing Well-Defined Polymers by Ruthenium-Catalyzed Living Radical Polymerization and Postreactions

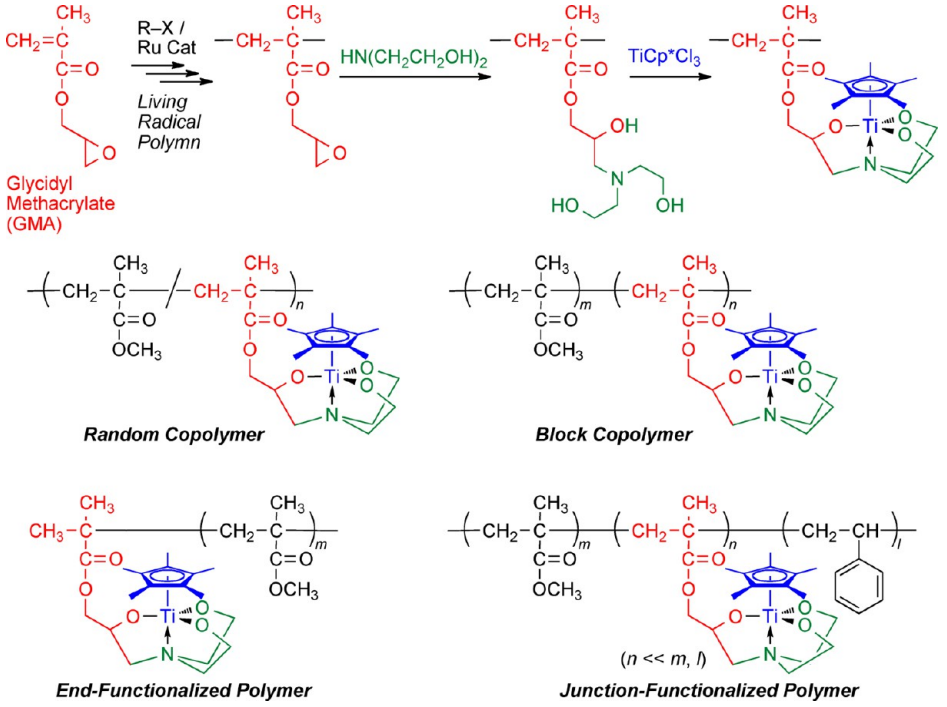

controlled/living radical polymerizations are one of the most promising methods for precision polymer synthesis.

In this study, we aimed to synthesize a series of titanium-containing well-defined random, block, and end-functionalized polymers via living radical polymerization. Titanium is the most abundant transition metal on Earth after iron and has been used in a wide variety of chemistry-related fields, such as pigments and catalysts. Although the well-controlled conjugation of titanium and organic polymers may provide various functions to polymeric materials, only a few published papers address the synthesis of well-defined titanium-containing hybrid polymers via the direct polymerization of titanium monomers or the polymerization of functionalized monomers followed by titanium loading via postreactions.[18−20] In contrast, comparatively many studies and synthetic methods have been reported for their iron counterparts.[1−4,21] Because titanium, just like the other metallic elements, shows characteristic electron energy losses upon irradiation of electron beam, it is possible to detect its distribution under electron microscopy combined with electron energy loss spectroscopy (EELS). Moreover, in combination with transmission electron microtomography (TEMT), three-dimensional (3D) elemental mapping of polymer microstructures can be obtained.[22−25]

Herein, the synthesis of well-defined titanium-containing random and block copolymers and end- and middle-functionalized polymers was achieved by the ruthenium-catalyzed living radical polymerization of glycidyl methacrylate (GMA) and postreactions with amino alcohols for the construction of ligating sites, followed by titanium complex loading via ligation with the pendent unit of the polymers (Scheme 1). Specifically, a discrete titanium-containing unit was successfully constructed in the desired position of the polymer chains by reacting the pendent epoxide with diethanolamine, which led to a tripodal structure consisting of three hydroxyethyl groups attached to a tertiary amino group, and reacting the resulting material with $TiCp^*Cl_3$ (Cp*: pentamethylcyclopentadienyl). The resultant Cp*-based titanatrane structure was highly stable to moisture. EELS, TEMT, and transmission electron microscopy (TEM) observations of the titanium-containing polymers revealed the presence of titanium-containing phases in the microphase-separated structure of the block copolymers.

RESULTS AND DISCUSSION

Ruthenium-Catalyzed Living Radical Homo- and Copolymerization of Glycidyl Methacrylate. GMA is one of most useful functionalized monomers for radical polymerization. The epoxy group, which is inert during the radical process, shows high reactivity to amines and other ionic species and is used to create polymeric materials such as coatings, resins, and adhesives. Although metal-catalyzed living radical polymerization or atom transfer radical polymerization of GMA has been primarily achieved using copper,[26−36] a few examples using ruthenium[13,37] have also been published. The latter is more suitable for methacrylates in terms of molecular weight control, and halogen end functionality can be obtained using the more stable carbon−chlorine dormant species.

We first examined the ruthenium-catalyzed living radical polymerization of GMA using a chloride initiator with a MMA dimer structure [H-$(MMA)_2$-Cl; MMA: methyl methacrylate] in conjunction with $Ru(Ind)Cl(PPh_3)_2$.[38−41] The polymerization occurred smoothly in toluene at 80 °C, reaching 80% conversion in 12 h. However, heterogeneous mixtures were produced due to the low solubility of poly(GMA) in toluene. Alternatively, in ethyl acetate, the polymerization proceeded homogeneously to produce polymers with well-controlled molecular weights, narrow molecular weight distributions (MWDs) (M_w/M_n = 1.1−1.2), and high monomer conversions (>90%, see Figure S1 of the Supporting Information).

We also investigated the random or statistical copolymerization of GMA and MMA using H-$(MMA)_2$-Cl/Ru(Ind)Cl-

dx.doi.org/10.1021/ma402332g | Macromolecules 2014, 47, 944−953

$(PPh_3)_2$ initiating systems. When small GMA feed ratios relative to MMA ($[MMA]_0/[GMA]_0$ = 3600/400 mM) were applied, the copolymerizations proceeded smoothly and homogeneously in toluene and both monomers were consumed at almost identical rates, resulting in random or statistical copolymers (Figure 1A). The polymers also showed narrow and unimodal size-exclusion chromatography (SEC) curves throughout the reaction. The number-average molecular weights (M_n) of the copolymers, which were obtained using poly(MMA) standard calibration for SEC, increased in direct proportion with the total monomer conversion and agreed well with the calculated values, assuming that one molecule of H-$(MMA)_2$-Cl generates one living copolymer chain (Figure 1B). These results indicate that the proposed ruthenium-based initiating system is quite effective for the living radical (co)polymerization of GMA under the appropriate conditions.

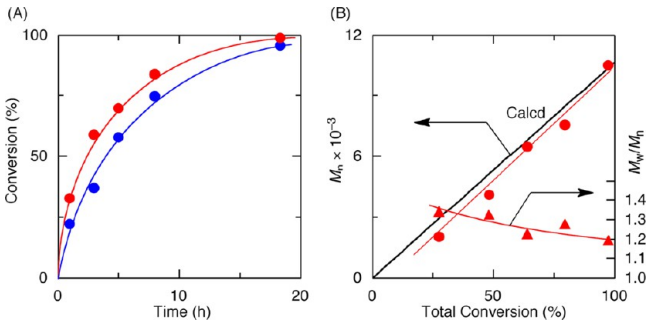

Figure 1. Living radical copolymerization of MMA and GMA in toluene at 80 °C: $[MMA]_0$ = 3.6 M; $[GMA]_0$ = 0.40 M; $[H\text{-}(MMA)_2\text{-}Cl]_0$ = 40 mM; $[Ru(Ind)Cl(PPh_3)_2]_0$ = 4.0 mM; $[n\text{-}Bu_3N]_0$ = 40 mM. (A) Conversion of GMA (red circles) and MMA (blue circles). (B) M_n (red circles) and M_w/M_n (red triangles) of the obtained copolymers.

Synthesis of Well-Defined Titanium-Containing Random Copolymers. The pendent epoxy groups in the copolymers were subjected to amination by various amino alcohols to introduce ligating sites for titanium. Three amino alcohols [2-(2-aminoethoxy)ethanol, *N*-(2-hydroxyethyl)-ethylenediamine, and diethanolamine] were used in excess with respect to the pendent epoxy groups to induce the complete ring-opening of the epoxy units, as will be confirmed by ^{1}H NMR (see below). The postreactions with the amino alcohols changed the solubility of the copolymers slightly to make their solubility in THF decreased. SEC characterization of the products in DMF gave unimodal SEC curves; however, a slight increase in the molecular weight and broadening in the MWD were observed due to the incorporation of pendent

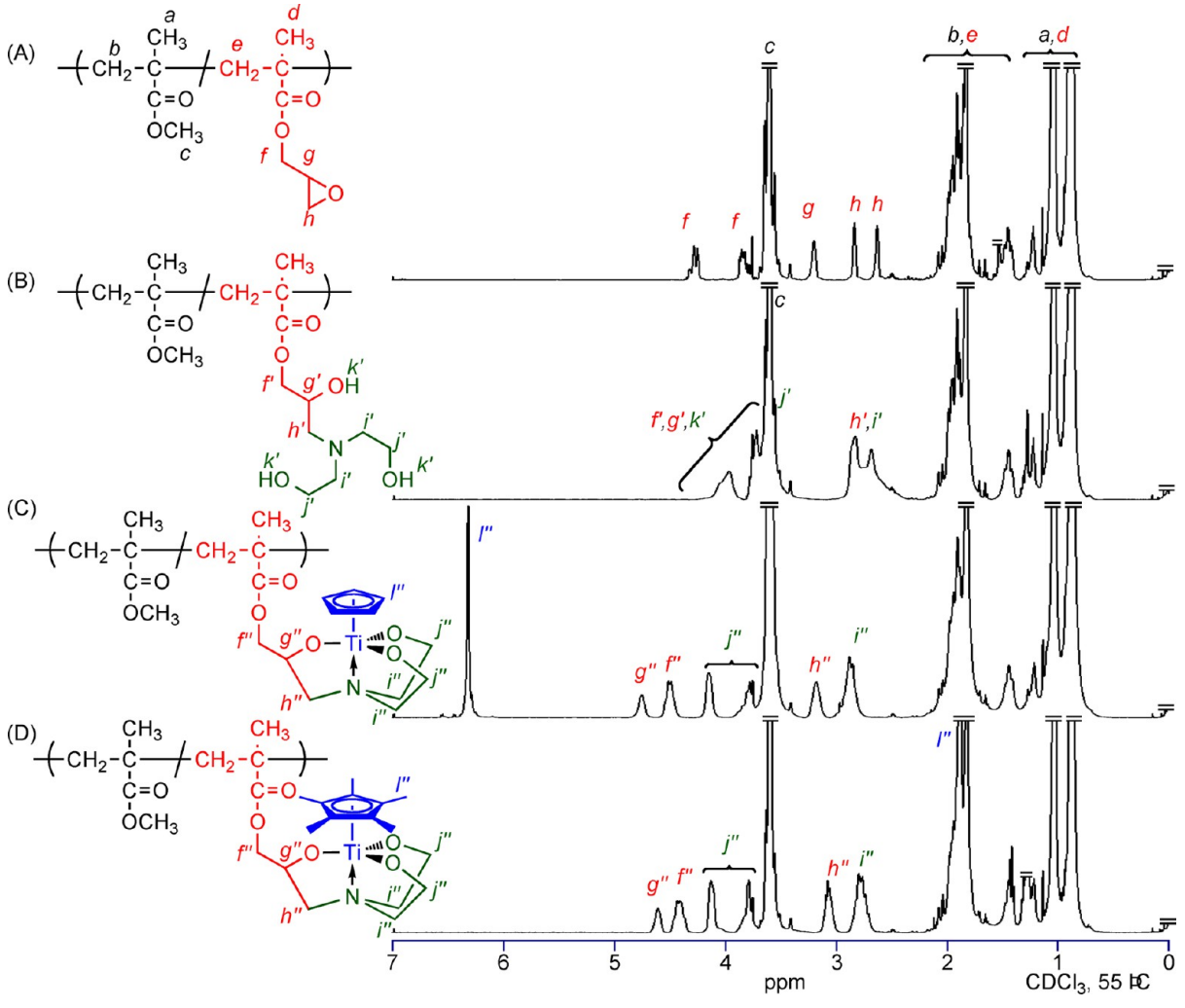

Figure 2. ^{1}H NMR spectra of poly(MMA-*co*-GMA) (A), copolymer reacted with diethanolamine (B), TiCp-loaded copolymer (C), and TiCp*-loaded copolymer (D) in $CDCl_3$ at 55 °C.

dx.doi.org/10.1021/ma402332g | *Macromolecules* 2014, 47, 944−953

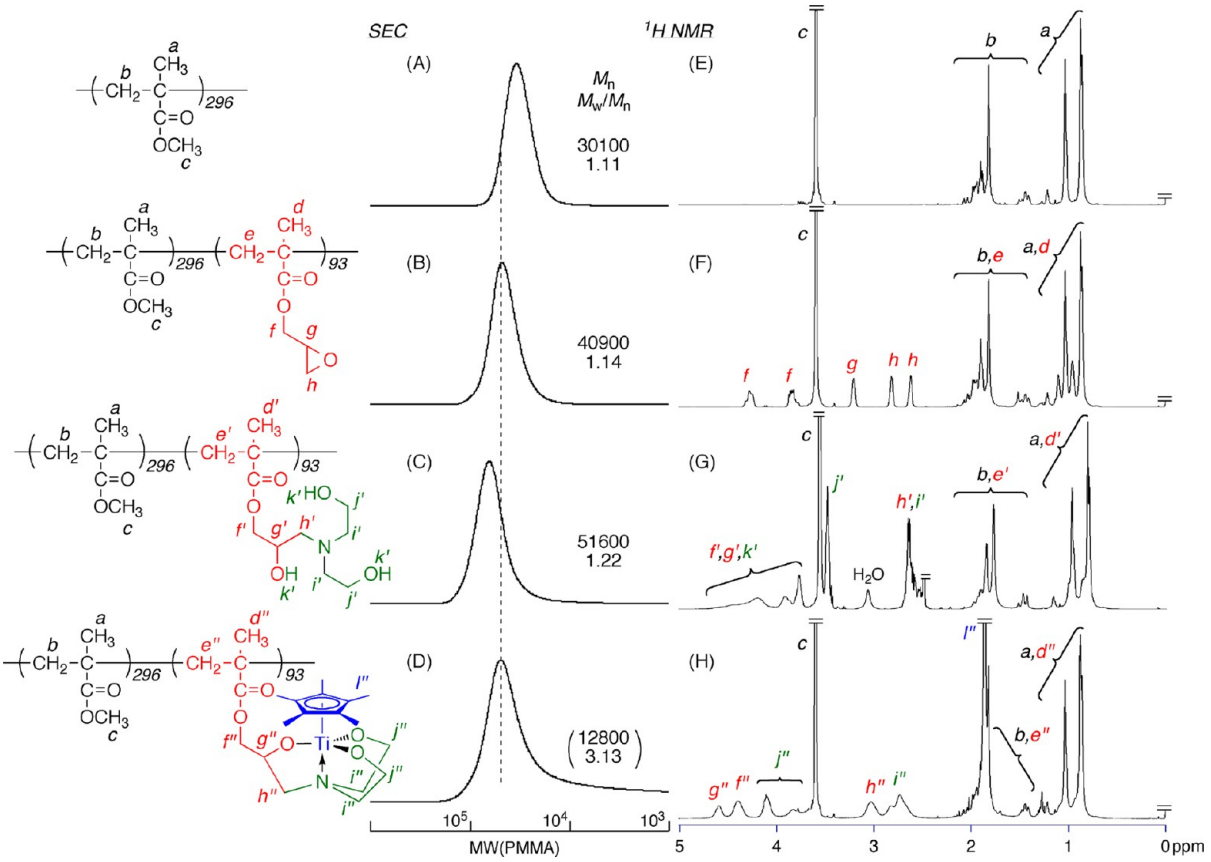

Figure 3. SEC curves and ^1H NMR spectra in $CDCl_3$ at 55 °C. (A, E) Poly(MMA) as macroinitiator obtained by ruthenium-catalyzed living radical polymerization of MMA ($[MMA]_0/[H\text{-}(MMA)_2\text{-}Cl]_0/[Ru(Ind)Cl(PPh_3)_2]_0/[n\text{-}Bu_3N]_0$ = 4000/9.3/1.5/40 mM) at 70% conversion in toluene at 80 °C. (B, F) Poly(MMA-*b*-GMA) obtained by ruthenium-catalyzed living radical block polymerization of GMA ($[GMA]_0/[C{-}Cl$ in macroinitiator$]_0/[Ru(Ind)Cl(PPh_3)_2]_0/[n\text{-}Bu_3N]_0$ = 1000/0.83/1.0/40 mM) at 23% conversion in toluene at 80 °C. (C, G) Block copolymer reacted with diethanolamine. (D, H) TiCp*-loaded block copolymer.

amino and hydroxy groups, which could interact with the packing materials in the SEC columns (see Figure S2 in the Supporting Information).

Upon further reacting with various titanium compounds [$Ti(OiPr)_4$, $TiCp_2Cl_2$, $TiCpCl_3$], the copolymers regained the solubility in THF, in which the SEC curves were measured. Specifically, the copolymers obtained from diethanolamine and $TiCpCl_3$ showed unimodal and narrow SEC curves, which had almost the same molecular weights as those of the starting MMA and GMA copolymers. Similar results were also obtained with $TiCp^*Cl_3$. In contrast, broad or unsymmetrical SEC curves were obtained with other aminoalcohols and $TiCpCl_3$ (Figure S2), and other titanium compounds led to the formation of insoluble products. The aforementioned results suggest that well-defined titanium-containing copolymers were obtained by the ruthenium-catalyzed living radical copolymerization of MMA and GMA followed by a simple postreaction with diethanolamine and $TiCpCl_3$ or $TiCp^*Cl_3$.

The copolymers produced via the postreactions with diethanolamine followed by $TiCpCl_3$ or $TiCp^*Cl_3$ were also analyzed by ^1H NMR spectroscopy (Figure 2). Upon the addition of diethanolamine to GMA-based copolymers, the characteristic glycidyl protons disappeared and different protons were observed, which were attributed to a ring-opened structure with tertiary amino groups attached to the three hydroxyethyl groups (Figure 2B). A series of characteristic peaks appeared after reaction with $TiCpCl_3$ or $TiCp^*Cl_3$ (denoted from *f″* to *j″* in Figures 2C,D). These peaks were assigned to discrete titanatrane structures, which are relatively stable titanium complexes that have been used as catalysts and in hybridization reactions with inorganic compounds.[42−50] The observed peak area ratios were close to the calculated values for titanatrane structures [*f″*:*g″*:*h″*:*i″*:*j″*/2 = 2.0:1:2.0:4.2:2.0 (for Cp), 2.0:1:2.0:4.1:2.2 (for Cp*), and 2:1:2:4:2 (calculated)]. These results clearly indicate that well-defined titanium-containing units were constructed in the copolymers.

To further confirm the stability of the titanatrane moiety in the copolymers, polymer solutions in $CHCl_3$ were mixed with water and the heterogeneous mixtures were vigorously stirred (400 rpm) for 20 days at room temperature. The SEC curves of the resultant CpTi-based copolymers show significant peak broadening, indicating that the titanium-containing structure decomposed (Figure S3A of the Supporting Information). In contrast, changes in the SEC curves were not detected for their Cp*Ti-based counterparts, even after the same treatment with water (Figure S3B). ^1H NMR analysis of the copolymers revealed that the Cp-titanatrane structures decomposed into the original tertiary amino alcohol moiety and cyclopentadiene, which was a byproduct originating from the titanium compound (Figure S4B). The high stability of the Cp*-titanatrane copolymers was also confirmed by ^1H NMR analysis, and spectral changes were not observed (Figure S4D). Changes in the residual titanatrane structures in the copolymers under hydrolytic conditions were analyzed using

dx.doi.org/10.1021/ma402332g | *Macromolecules* 2014, 47, 944−953

the ^{1}H NMR spectra of the copolymers over time. As shown in Figure S5, the Cp*-based titanatrane structure of the copolymers and model compound, which was prepared from glycidyl pivalate, diethanolamine, and TiCp*Cl_3, was highly stable to hydrolysis, in contrast to the Cp counterpart. The high stability of Cp*-based titanatrane structures was also observed in [Cp*Ti(N($CH_2CH_2O)_3$)], a previously reported Cp*-titanatrane catalyst that showed relatively high activity for the syndiospecific coordination polymerization of styrene.[46,47] These results prompted us to synthesize a series of stable, well-defined titanium-containing copolymers using the glycidyl unit, diethanolamine, and TiCp*Cl_3.

Synthesis of Titanium-Containing Diblock Copolymers. The synthesis of titanium-containing diblock copolymers was performed using a strategy based on the ruthenium-catalyzed block copolymerization of MMA and GMA and postreactions with diethanolamine and TiCp*Cl_3. For this purpose, the living radical polymerization of MMA was carried out with H-$(MMA)_2$-Cl/Ru(Ind)Cl$(PPh_3)_2$/n-Bu_3N to produce well-defined poly(MMA)s with controlled molecular weights (M_n = 30 100, M_w/M_n = 1.11) and chlorine chain ends (Figure 3A). The isolated polymer by precipitation (M_n = 29 600, M_w/M_n = 1.12) was used as a macroinitiator for the ruthenium-catalyzed living radical block polymerization of GMA in ethyl acetate. The SEC curves of the copolymers shifted to high molecular weights, and narrow MWDs (M_n = 40 900, M_w/M_n = 1.14) were maintained as the polymerization proceeded (Figure 3B). The M_n(NMR) obtained by ^{1}H NMR was 42 800, which is close to the calculated value and the SEC results. The number-average degrees of polymerization (DP_n) of MMA and GMA units obtained by ^{1}H NMR were 296 and 93, respectively (Figure 3F). Thus, ruthenium-catalyzed living radical polymerization was effective for the synthesis of well-defined MMA and GMA diblock copolymers.

Block copolymers containing glycidyl moieties were treated with diethanolamine and were converted to polymers with aminoalcohol-based ligands as pendent groups in the block segments. The SEC curves of the copolymers shifted to higher molecular weights, and narrow MWDs were maintained, even after the reaction was performed (Figure 3C). The quantitative amination of glycidyl groups was confirmed by ^{1}H NMR analysis (Figure 3G). Subsequent reaction with TiCp*Cl_3 resulted in the formation of titanium-containing block copolymers, as confirmed by the corresponding changes in the signals of the ^{1}H NMR spectrum (Figure 3H). Although the peak of the SEC curve of the copolymers was sharp and unimodal and shifts were not observed, tailing occurred due to the interaction of titanium-containing block segments with the column packing materials (Figure 3D). These results indicate that the above procedures successfully synthesized well-defined titanium-containing block copolymers.

Synthesis of Titanium-Containing Junction-Functionalized Block Copolymers. The method was also applied to the synthesis of block copolymers of MMA and styrene with junctions containing titanium parts. The ruthenium-catalyzed living radical polymerization of MMA (667 equiv with respect to the chloride initiator [H-$(MMA)_2$-Cl]) was conducted with H-$(MMA)_2$-Cl/Ru(Ind)Cl$(PPh_3)_2$/n-Bu_3N to produce living poly(MMA) (M_n = 44 000, M_w/M_n = 1.12) at 75% conversion (Figure 4A), into which a small amount of GMA (25 equiv to the initiator) was added. When the conversion of MMA and GMA reached 76% and 48%, respectively, the polymerization was stopped to obtain block copolymers consisting of

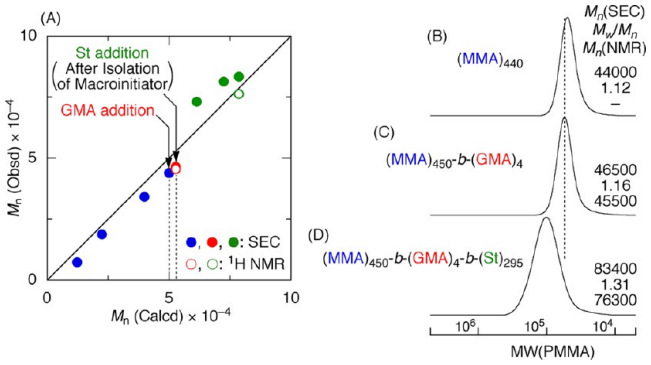

Figure 4. Synthesis of precursor for junction-functionalized polymers via ruthenium-catalyzed living radical polymerization of MMA ($[MMA]_0/[H\text{-}(MMA)_2\text{-}Cl]_0/[Ru(Ind)Cl(PPh_3)_2]_0/[n\text{-}Bu_3N]_0$ = 3600/5.4/1.0/10 mM) followed by sequential addition of GMA ($[GMA]_{add}$ = 140 mM) and subsequent living radical block polymerization of styrene initiated from the macroinitiator of poly(MMA-b-GMA) thus obtained ($[St]_0/[C\text{–}Cl$ in macroinitiator$]_0/[RuCp^*Cl(PPh_3)_2]_0/[n\text{-}Bu_3N]_0$ = 4000/2.0/1.0/10 mM) in toluene at 80 °C. (A) M_n obtained by SEC (blue, red, and green filled circles) and ^{1}H NMR (red and green open circles). SEC curves of poly(MMA) (B), poly(MMA-b-GMA) (C), and poly(MMA-b-GMA-b-St) (D). For simplicity, the obtained block copolymers, $((MMA)_{440}\text{-}b\text{-}[(MMA)_{9.5}\text{-}co\text{-}(GMA)_{4.2}])$ and $((MMA)_{440}\text{-}b\text{-}[(MMA)_{9.5}\text{-}co\text{-}(GMA)_{4.2}]\text{-}b\text{-}(St)_{295})$, are denoted as $(MMA)_{450}\text{-}b\text{-}(GMA)_4$ and $(MMA)_{450}\text{-}b\text{-}(GMA)_4\text{-}b\text{-}(St)_{295}$, respectively.

poly(MMA) and short segments GMA and MMA copolymers with narrow MWDs (M_n = 46 500, M_w/M_n = 1.16) (Figure 4B). ^{1}H NMR analysis of the isolated copolymers showed that short blocks consisting of 4.2 units of GMA and 9.5 units of MMA were produced, and the DP_n of poly(MMA) segments was estimated as 440 using the molecular weight of the prepolymer of MMA [M_n(SEC) = 44 000]. The copolymer was then used as a macroinitiator for the ruthenium-catalyzed living radical block polymerization of styrene (2000 equiv with respect to the macroinitiator) using RuCp*$Cl(PPh_3)_2$, as previously reported.[51] When the conversion of styrene reached 16%, the polymerization was terminated to produce styrene-blocked copolymers with controlled molecular weights [M_n(SEC) = 83 400, M_w/M_n = 1.31] (Figure 4C). A DP_n of 295 was calculated for the polystyrene segments using the peak intensity ratios of the ^{1}H NMR spectrum of the copolymers. Thus, block copolymers consisting of outer poly(MMA) (m = 440) and polystyrene (l = 295) segments with short segments of copolymers of MMA (m' = 10) and GMA (n = 4) units at the junction of poly(MMA) and polystyrene were produced. The M_n of the copolymers, which was determined by SEC and ^{1}H NMR, agreed with the calculated values obtained during the polymerization and increased as the polymerization proceeded (Figure 4D).

Block copolymers containing GMA units were treated with diethanolamine followed by CpTiCl_3 or Cp*TiCl_3 to produce block copolymers containing titanatrane units at the junction of poly(MMA) and polystyrene. The successful synthesis was confirmed using SEC and ^{1}H NMR analysis (Figures S6 and S7).

Synthesis of Titanium-Containing End-Functionalized Polymers. Cp*-based titanatrane chemistry was also applied in conjunction with the ruthenium-catalyzed living radical polymerization of MMA with a functionalized initiator to synthesize titanium end-functionalized polymers. For this

dx.doi.org/10.1021/ma402332g | Macromolecules 2014, 47, 944–953

approach, we synthesized a glycidyl-functionalized initiator with a reactive carbon−halogen bond by reacting 2-bromoisobutyryl bromide with glycidol.[52] The initiator was then employed as an end-functionalized initiator for the living radical polymerization of MMA in the presence of $Ru(Ind)Cl(PPh_3)_2$ as the catalyst in toluene at 80 °C. The polymerization occurred smoothly and resulted in the formation of polymers with narrow MWDs (M_w/M_n = 1.1−1.2) and well-controlled molecular weights, which increased in direct proportion with the monomer conversion (Figure 5).

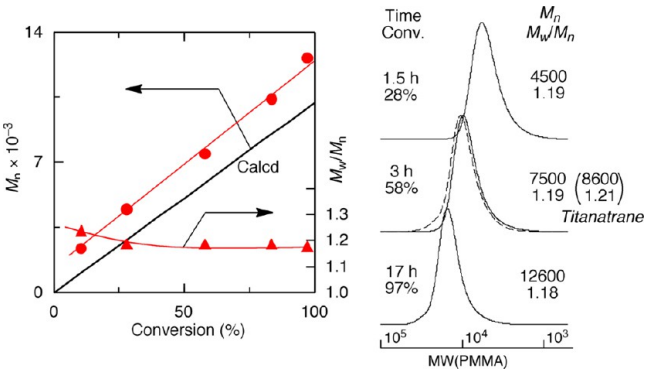

Figure 5. Synthesis of glycidyl end-functionalized poly(MMA) by living radical polymerization of MMA with H-GMA-Br in toluene at 80 °C: $[MMA]_0$ = 4.0 M; $[H\text{-}GMA\text{-}Br]_0$ = 40 mM; $[Ru(Ind)Cl(PPh_3)_2]_0$ = 1.0 mM; $[n\text{-}Bu_3N]_0$ = 10 mM. (A) Conversion of MMA (red circles). (B) M_n (red circles) and M_w/M_n (red triangles) of the obtained polymers.

^1H NMR analysis was used to determine the functionality of the epoxy group at the chain end. A series of signals originating from the glycidyl moiety were observed at chemical shifts similar to those of the random GMA copolymers; however, the relative intensity was much lower for the end-functionalized polymers (Figure S8A). The M_n of the polymers, which was determined using the peak intensity ratio of the epoxy groups (*e*) and the main-chain methyl ester units, was 7800, which was very close to the value obtained by SEC calibrated with poly(MMA) standards. The end functionality of the epoxy unit was 0.98, indicating the formation of well-defined end-functionalized polymers.

The epoxy rings in the end-functionalized polymers were opened with diethanolamine and were quantitatively converted to the corresponding aminoalcohol units (Figure S8B). $TiCp^*Cl_3$ was added to the ligands to produce titanium end-functionalized poly(MMA) with narrow MWDs (dotted line in Figure 5). In the resulting polymers, the chain end functionality (F_n = 0.99) was almost identical to that of the epoxy end-functionalized polymers. Thus, a strategy based on glycidyl units, diethanolamine, and $TiCp^*Cl_3$ in conjunction with ruthenium-catalyzed living radical polymerization was quite effective for synthesizing well-defined titanium end-functionalized polymers.

Electron Energy Loss Spectroscopy, Transmission Electron Microscopy, and Microtomography of Titanium-Containing Block Copolymers. The nanostructures of titanium-containing block copolymers were investigated using EELS, TEM, and TEMT. The EELS analysis of polymer films of titanium-containing diblock copolymers, which were synthesized from block copolymers of MMA and GMA [$(MMA)_m$-*b*-$(GMA)_n$; m = 296, n = 93; M_n(SEC) = 42 800, M_w/M_n = 1.14], showed characteristic electron energy loss at approximately 456 eV, which was assigned to the L-edge core-loss peak of titanium (Figure S9B). As expected, the peak intensities increased with increasing thickness of the ultrathin section. These results indicate that titanium was incorporated into the cast film of the copolymers and that leaching did not occur during the film preparation procedures.

In order to map titanium in the specimens, the three-window method was employed (Figure S10).[53,54] The titanium map was obtained by subtracting the background image, which was constructed from two pre-edge images (406 ± 20 and 426 ± 20 eV) and one postedge image (481 ± 20 eV). The titanium-containing part corresponded to the green dots in Figure 6A and was clearly located in microphase-separated lamellae or cylindrical structures with a size of 19 nm.

TEMT is combined with EELS (hereafter we call the method TEMT-EELS for simplicity) is one of the best methods for identifying titanium-containing domains in 3D. Note here that more than 100 TEM micrographs are taken by tilting a specimen during TEMT experiment. In the case of TEMT-EELS with three window methods involves three exposures at each tilt angle, making the total number of TEM micrographs would be more than 300. Thus, it would require ca. 5 h to perform TEMT-EELS with the three-window method, most probably causing severe electron beam damage to the specimen. It is therefore impractical for us to perform such TEMT-EELS.

Instead, although not so rigorous as the three-window method, we may use low-loss electron imaging for elemental mapping. The biggest advantage of using such low-loss EELS imaging is that a single exposure is only necessary to take

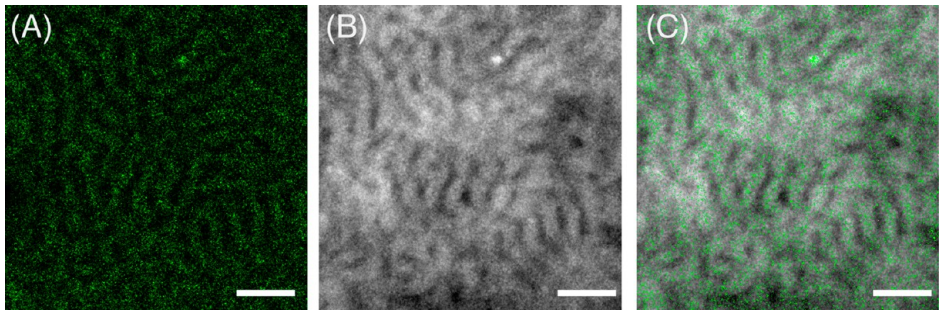

Figure 6. (A) Titanium map obtained by three-window method around core-loss L-edge (456 eV) of titanium, (B) low-loss image (45 ± 5 eV), and (C) superimposed image of (A) and (B) for the specimen with a 30 nm thickness of the titanium-containing diblock copolymers obtained from the block copolymers of MMA and GMA [$(MMA)_m$-*b*-$(GMA)_n$; m = 296, n = 93; M_n(SEC) = 42 800, M_w/M_n = 1.14]. The scalar bar shows 50 nm.

dx.doi.org/10.1021/ma402332g | *Macromolecules* 2014, 47, 944−953

elemental mapped image at each tilt angle, dramatically reducing the electron beam damage of the sample. In the low-loss region where the electron energy loss is smaller than approximately 50 eV, the electrons that have induced plasmon oscillations occur. Because the plasmon generation is the most frequent inelastic interaction of electron with the sample, the intensity in this low-loss region is relatively high. Intensity and number of plasmon peaks increase with specimen thickness. Titanium is known to have absorption at low-loss energies around 48 eV. In fact, the EELS of the specimens showed shoulders at approximately 48 eV (Figure S9C), and the intensities increased with increasing thickness of the ultrathin section.

A series of filtered images at low-loss energies were measured from 0 to 60 eV (Figures S11A–H). The image obtained at 45 ± 5 eV clearly showed the microphase-separated structure of the material (see Figure S11F and Figure 6B). The TEM low-loss EELS image (Figure 6B) as described above was superimposed on the titanium map (Figure 6A), as shown in Figure 6C, and white or bright domains overlaid perfectly on the green dots of the titanium map.

Three ultrathin sections with different thicknesses (30, 50, and 90 nm) were examined using the low-loss EELS method (45 ± 5 eV) at a 50° tilt angle (Figure S12). The 90 nm specimen was too thick to observe because of the increased background intensity, while the thinnest specimen (30 nm) produced blurred images due to insufficient number of electrons, i.e., low counting statistics. The sample with a moderate thickness of 50 nm was best suited for the 3D construction. In fact, because the periodicity of the system is 19 nm, 50 nm thick specimen gives better 3D representation of the morphology than the 30 nm thick specimen. Thus, we obtained a series of low-loss images (45 ± 5 eV) of the 50 nm specimen by tilting the ultrathin section from −60° to 60° in 2° increments. Figure 7 displays the reconstructed 3D image clearly demonstrating the microphase-separated continuous morphology. Therefore, the titanium-containing copolymers were also arranged in the highly stable microphase-separated structure similarly to that of the block copolymers without the metal.

Although EELS was also conducted for the triblock copolymers possessing a short segment of titanium containing units at the junction between poly(MMA) and polystyrene segments, the absorption of the L-edge was too low to analyze the titanium-containing part. TEM analysis of the junction of poly(MMA) and polystyrene segments with titanium-containing parts was difficult due to the lower content of titanium in the triblock copolymers. However, the microphase-separated morphology and lamellae structure were observed by staining the polystyrene segments with RuO_4 (Figure 8),[55] even in poly(MMA) and polystyrene segments in the block copolymer containing titanium in the junction [M_n(SEC) = 74 900, M_w/M_n = 1.42, m = 440, l = 295, m' = 10, n = 4; the same sample is shown in Figure 5D].

CONCLUSIONS

In conclusion, a series of well-defined titanium-containing random, block, end-functionalized, and junction-functionalized polymers were successfully prepared by combining ruthenium-catalyzed living radical polymerization and glycidyl moieties, which were subsequently reacted with diethanolamine and $TiCp^*Cl_3$ to produce stable titanatrane units. Titanium-containing domains in microphase-separated block copolymers

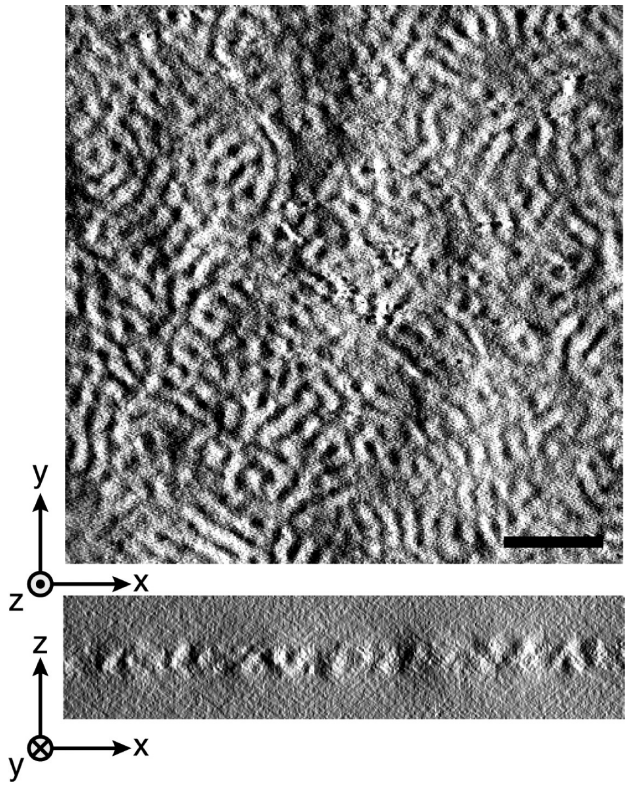

Figure 7. (A) Two-dimensional planar (x, y) and cross-sectional (x, z) slices of the morphologies as observed by 3D TEMT at low loss (45 ± 5 eV) and (B) 3D solid renditions for the specimen with a 50 nm thickness of the titanium-containing diblock copolymers obtained from the block copolymers of MMA and GMA [$(MMA)_m$-b-$(GMA)_n$; m = 296, n = 93; M_n(SEC) = 42 800, M_w/M_n = 1.14]. The bright regions are corresponding to the titanium-containing GMA part. The scale bar shows 100 nm.

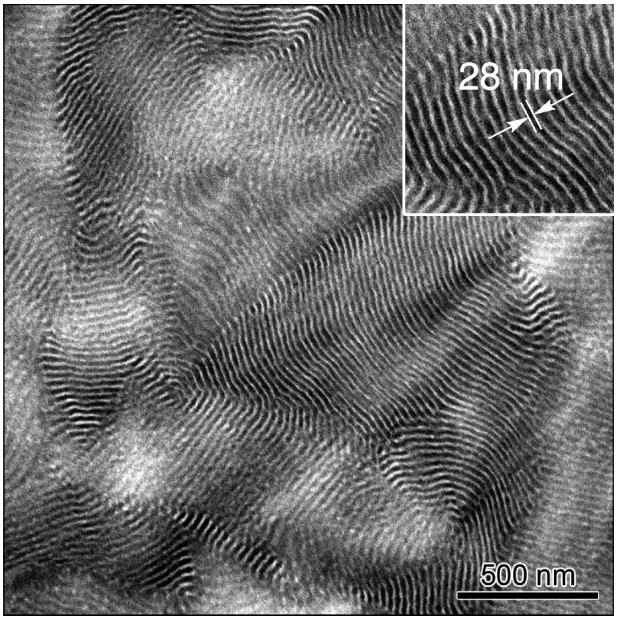

Figure 8. TEM image of the RuO_4-stained triblock copolymer containing a short segment of the titanium containing units [$(MMA)_m$-b-[$(MMA)_{m'}$-co-(TiCp*-loaded $GMA)_n$]-b-$(St)_l$; m = 440, m' = 10, n = 4, l = 295; M_n(SEC) = 74 900, M_w/M_n = 1.42].

dx.doi.org/10.1021/ma402332g | Macromolecules 2014, 47, 944–953

were directly observed by EELS. 3D images of the titanium-containing domains were constructed using low-loss EELS TEMT images. The proposed synthetic method based on glycidyl units, diethanolamine, and $TiCp^*Cl_3$ is a unique and novel strategy for producing titanium-containing, well-defined polymers.

EXPERIMENTAL SECTION

Materials. MMA (Tokyo Kasei, >98%), GMA (Tokyo Kasei, >95%), styrene (Wako Chemicals, >98%), diethanolamine (Tokyo Kasei, >99%), 2-(2-aminoethylamino)ethanol (Tokyo Kasei, >99%), and 2-(2-aminoethoxy)ethanol (Tokyo Kasei, >98%) were distilled from calcium hydride under reduced pressure before use. Tributylamine (Tokyo Kasei, >98%) and triethylamine (Tokyo Kasei, >99%) were distilled from calcium hydride before use. $Ru(Ind)Cl(PPh_3)_2$, $RuCp^*Cl(PPh_3)_2$ (provided from Wako Chemicals), $TiCpCl_3$ (Aldrich, >97%), and $TiCp^*Cl_3$ (Tokyo Kasei, >97%) were used as received. All metal compounds were handled in a glovebox (VAC Nexus) under a moisture- and oxygen-free argon atmosphere (O_2, <1 ppm). $Me_2C(CO_2Me)CH_2C(CO_2Me)(Me)Cl$ H-$(MMA)_2$-Cl] was prepared according to the literature.[39] Toluene (Kanto, >99.5%; H_2O < 10 ppm) was dried and deoxygenized by passage through columns of Glass Contour Solvent Systems before use.

Synthesis of H-GMA-Br. H-GMA-Br was synthesized from 2-bromoisobutyryl bromide (TCI; >98%) and glycidol (KANTO; >95%). The reaction was carried out with the use of a syringe technique under a dry argon atmosphere in an oven-dried glass tube equipped with three-way stopcocks. 2-Bromoisobutyryl bromide (25.5 mL, 0.20 mol) was added dropwise with vigorous stirring to a solution of glycidol (13.2 mL, 0.20 mol) and triethylamine (30.5 mL, 0.22 mol) in dry THF (29.4 mL) at 0 °C. The mixture was kept stirring for 2 h at 0 °C and then over 14 h at room temperature. After the dilution with diethyl ether, the mixture was washed with saturated NaCl aqueous solution and water. The ether solution was dried on $MgSO_4$ and evaporated to dryness under reduced pressure. The product was distilled over calcium hydride under reduced pressure to give pure H-GMA-Br (19.2 g, 0.086 mol; yield = 43.0%). ^1H NMR ($CDCl_3$, rt): δ 1.96 (s, 6H, CH_3), 2.72 (dd, 1H, *gem*-CH_2), 2.87 (dd, 1H, *gem*-CH_2), 3.26 (m, 1H, CH), 4.07 (dd, J_{vic} = 5.9 Hz, J_{gem} = 12.1 Hz, 1H, *gem*-CH_2), 4.50 (dd, J_{vic} = 2.8 Hz, J_{gem} = 12.1 Hz, 1H, *gem*-CH_2).

Living Radical Copolymerization of GMA and MMA. All polymerizations were carried out by syringe technique under dry nitrogen in glass tubes equipped with a three-way stopcock or in baked and sealed glass vials. A typical example for the copolymerization of GMA and MMA with H-$(MMA)_2$-Cl/$Ru(Ind)Cl(PPh_3)_2$/*n*-Bu_3N is given below. In a 50 mL round-bottomed flask was placed $Ru(Ind)Cl(PPh_3)_2$ (21.7 mg, 0.028 mmol), toluene (2.8 mL), MMA (2.7 mL, 25.2 mmol), GMA (0.37 mL, 2.8 mmol), H-$(MMA)_2$-Cl (0.46 mL of 604 mM solution in toluene, 0.28 mmol), and *n*-Bu_3N (0.7 mL of 400 mM solution in toluene, 0.28 mmol) at room temperature. The total volume of reaction mixture was 7.0 mL. Immediately after mixing, six aliquots (1.0 mL each) of the solutions were injected into backed glass tubes. The reaction vials were sealed and placed in an oil bath kept at 80 °C. In predetermined intervals, the polymerization was terminated by cooling the reaction mixtures to −78 °C. Monomer conversions determined by gas chromatography with toluene as an internal standard reached 96% for MMA and 99% for GMA for 18 h, respectively. The quenched reaction mixture was diluted with toluene (ca. 20 mL) and rigorously shaken with an absorbent [Kyowaad-2000G-7 ($Mg_{0.7}Al_{0.3}O_{1.15}$); Kyowa Chemical] (~5 g) to remove the metal-containing residues. After the absorbent was separated by filtration, the filtrate was washed with aqueous citric acid solution and water, evaporated to dryness under reduced pressure, and vacuum-dried to give the product copolymer (M_n = 10 500, M_w/M_n = 1.20). The incorporation units of MMA and GMA in the obtained copolymer were estimated at 91 and 11, respectively, by ^1H NMR.

Synthesis of Titanium-Containing Polymer from Poly(GMA-*co*-MMA). The titanium-containing polymers were prepared by treating GMA-containing copolymers with multidentate primary or secondary amines followed by complexation with titanium compounds under a dry argon atmosphere in an oven-dried glass tube equipped with three-way stopcocks. A typical example for the introduction of titanatrane into MMA/GMA random copolymer is given below. The MMA/GMA (9/1) random copolymer (4.0 g) obtained with the $Ru(Ind)Cl(PPh_3)_2$ system was dissolved in dry THF (93 mL). Into the solution, diethanolamine (52 mL, 150 equiv to GMA units) was added at 60 °C and stirred for 85 h. After the reaction, the reaction mixture was dialyzed in methanol for 3 days and was then evaporated to remove the solvents. The obtained crude product was redissolved in small amount of ethanol and precipitated from *n*-hexane to give the copolymer with pendent amino and hydroxyl groups (3.5 g, 80% yield). The obtained copolymer with the multidentate ligands was then treated with titanium compounds. The copolymer (1.0 g), 0.27 g of $TiCp^*Cl_3$ (1.1 equiv to GMA units), and 0.7 mL of triethylamine (6.0 equiv) were dissolved in $CHCl_3$ (99 mL) and stirred at room temperature for 22 h. The reaction mixture was precipitated from *n*-hexane, and the precipitate was redissolved in $CHCl_3$, washed with water 3 times, dried on $MgSO_4$, and precipitated from *n*-hexane again to afford titanium-containing polymer as yellowish solid (M_n = 10 900, M_w/M_n = 1.21).

Stability Test of Titanium-Containing Polymer for Water. The titanium-containing polymer was placed in a 100 mL round-bottom flask equipped with three-way stopcocks and dissolved in 15 mL of $CDCl_3$. Into the flask, 30 mL of distilled and degassed water was added, and the heterogeneous mixture was vigorously stirred at room temperature for 20 days. The stability of the titanium complex was monitored by using ^1H NMR and SEC measurements.

Synthesis of Titanium-Containing Block Copolymers. Titanium-containing block copolymers were prepared via ruthenium-catalyzed living radical block copolymerization followed by transformation of the GMA units into titanatrane. A typical example for the synthesis of a titanium-containing diblock copolymer is given below. In a 50 mL round-bottomed flask was placed $Ru(Ind)Cl(PPh_3)_2$ (67.4 mg, 0.0868 mmol), toluene (31.5 mL), MMA (24.8 mL, 232 mmol), H-$(MMA)_2$-Cl (1.0 mL of 530 mM solution in toluene, 0.53 mmol), and *n*-Bu_3N (0.55 mL, 2.32 mmol) at room temperature. The total volume of reaction mixture was 57.9 mL. The flask was placed in an oil bath kept at 80 °C under stirring for 32 h, and the polymerization was quenched at 70% conversion by cooling the reaction mixtures to −78 °C. The quenched reaction mixture was diluted with toluene (ca. 20 mL) and rigorously shaken with an absorbent [Kyowaad-2000G-7 ($Mg_{0.7}Al_{0.3}O_{1.15}$)] to remove the metal-containing residues. The mixture was precipitated into hexane, isolated by centrifugation, and measured by SEC (M_n = 30 100, M_w/M_n = 1.11). The precipitate was diluted with THF and precipitated from hexanes. The procedure was repeated three times. The precipitate was then evaporated to dryness to yield the PMMA with Cl terminal, which was subsequently employed as the macroinitiator for the block copolymerization (15.0 g, 92% yield; M_n = 29 600, M_w/M_n = 1.11). The block copolymerization of GMA from the PMMA macroinitiator was also conducted with the $Ru(Ind)Cl(PPh_3)_2$ system as follows. In a 50 mL round-bottomed flask was placed PMMA macroinitiator (3.7 g, 0.125 mmol C−Cl bond), GMA (6.64 mL, 50.0 mmol), $Ru(Ind)Cl(PPh_3)_2$ (155 mg, 0.20 mmol), and *n*-Bu_3N (0.48 mL, 2.00 mmol) at room temperature. The total volume of reaction mixture was 50 mL. The flask was placed in an oil bath kept at 80 °C under stirring for 1.5 h, and the polymerization was quenched at 23% conversion by cooling the reaction mixtures to −78 °C. The quenched reaction mixture was diluted with toluene (ca. 20 mL) and rigorously shaken with an absorbent [Kyowaad-2000G-7 ($Mg_{0.7}Al_{0.3}O_{1.15}$)] to remove the metal-containing residues. The mixture was precipitated into hexane, isolated by centrifugation, and measured by SEC (M_n = 40 900, M_w/M_n = 1.14). The precipitate was diluted with THF and precipitated from hexanes. After three times precipitation, the precipitate was evaporated to dryness to yield the MMA-*b*-GMA diblock copolymer, which was subsequently employed as precursor for the titanium-containing block copolymers (5.18 g, 97% yield; M_n = 40 600, M_w/M_n = 1.15). The M_n(NMR) was also calculated by peak area ratios of MMA (peak *c*) and GMA (peaks *g*

dx.doi.org/10.1021/ma402332g | *Macromolecules* 2014, 47, 944−953

and *h*) units in the ^{1}H NMR spectrum (Figure 3F) and M_n of the prepolymer of MMA by SEC (M_n = 29 600) to be 42 800. The GMA unit in the obtained copolymer was converted into titanatrane by the same procedure for the aforementioned random copolymer to afford a titanium-containing block copolymer. The titanium-containing junction-functionalized block copolymers were also prepared by the similar sequential block copolymerization using ruthenium complexes.

Synthesis of Titanium-End-Functionalized Polymer. Titanium-end-functionalized polymer was also prepared via ruthenium-catalyzed living radical polymerization using H-GMA-Br as the initiator, which was followed by the transformation of GMA units into titanatrane. A typical example for the synthesis of the end-functionalized PMMA with H-GMA-Br/Ru(Ind)Cl(PPh_3)$_2$/*n*-Bu_3N is given below. In a 50 mL round-bottomed flask was placed Ru(Ind)Cl(PPh_3)$_2$ (40.4 mg, 0.052 mmol), toluene (25.0 mL), MMA (22.2 mL, 208 mmol), H-GMA-Br (3.4 mL of 614 mM solution in toluene, 2.08 mmol), and *n*-Bu_3N (1.3 mL of 400 mM solution in toluene, 0.520 mmol) at room temperature. The total volume of reaction mixture was 52.0 mL. The flask was placed in an oil bath kept at 80 °C under stirring for 3 h, and the polymerization was quenched at 58% conversion by cooling the reaction mixtures to −78 °C. The quenched reaction mixture was diluted with toluene (ca. 20 mL) and rigorously shaken with an absorbent [Kyowaad-2000G-7 ($Mg_{0.7}Al_{0.3}O_{1.15}$)] to remove the metal-containing residues. The mixture was precipitated into hexane and isolated by centrifugation. The precipitate was diluted with THF and precipitated from hexanes. After three times precipitation, the precipitate was evaporated to dryness to yield the PMMA with a GMA terminal unit (11.1 g, 70% yield; M_n = 7700, M_w/M_n = 1.19). The terminal GMA unit in the obtained polymer was converted into titanatrane by the aforementioned procedure to afford a titanium-end-functionalized polymer.

Measurements. Monomer conversion was determined from the concentration of residual monomer measured by ^{1}H NMR spectroscopy with toluene as an internal standard. ^{1}H NMR spectra were recorded on a JEOL ECS-400 spectrometer, operating at 400 MHz. The number-average molecular weight (M_n) and the molecular weight distribution (M_w/M_n) of the product polymers were determined by size-exclusion chromatography (SEC) in THF at 40 °C on two polystyrene gel columns [Shodex KF-805 L (pore size: 20−1000 Å; 8.0 mm i.d. × 30 cm) × 2; flow rate 1.0 mL/min] connected to a JASCO PU-2080 precision pump and a JASCO RI-2031 detector. The columns were calibrated against 8 standard poly(MMA) samples (Shodex; M_p = 202−1 950 000; M_w/M_n = 1.02−1.09). The film specimens for TEM, EELS, and TEMT-EELS experiments were prepared by casting 5 wt % toluene solutions at room temperature. The obtained films were ultramicrotomed to thicknesses of 30, 50, and 90 nm using an Ultracut UCT microtome (Leica, Germany) with a diamond knife at room temperature. TEM, EELS, and TEMT-EELS experiments were carried out on an energy filter installed JEM-2200FS (JEOL Ltd., Japan) operated at 200 kV and equipped with a slow-scan USC 4000 CCD camera (Gatan, Inc.). A series of low-loss images in TEMT-EELS were acquired at tilt angles in the range of −60° to 60° at an angular interval of 2°. The tilt series of the low-loss images after the alignment by the fiducial marker method[56] were reconstructed by filtered back-projection.[57]

■ ASSOCIATED CONTENT

Ⓢ Supporting Information

Polymerization results, SEC curves, ^{1}H NMR spectra, electron energy loss spectra, and energy filter images of the specimen of the polymers. This material is available free of charge via the Internet at http://pubs.acs.org.

■ AUTHOR INFORMATION

Corresponding Authors

*E-mail satoh@apchem.nagoya-u.ac.jp (K.S.).
*E-mail hjinnai@cstf.kyushu-u.ac.jp (H.J.).
*E-mail kamigait@apchem.nagoya-u.ac.jp (M.K.).

Notes

The authors declare no competing financial interest.

■ ACKNOWLEDGMENTS

This work was supported in part by a Grant-in-Aid for Scientific Research on Innovative Areas "Fusion Materials (Creative Development of Materials and Exploration of their Function through Molecular Control; Area No. 2203)" (No. 23107515) for K.S. from the Ministry of Education, Culture, Sports, Science and Technology, Japan, and the Global COE Program "Elucidation and Design of Materials and Molecular Functions". H.J. is grateful to the Ministry of Education, Science, Sports and Culture through Grants-in-Aid No. 24310092.

■ REFERENCES

(1) *Frontiers in Transition Metal-Containing Polymers*; Abd-El-Aziz, A. S., Manners, I., Eds.; Wiley-Interscience: Hoboken, NJ, 2007.
(2) Manners, I. *Synthetic Metal-Containing Polymers*; Wiley-VCH: Weinheim, Germany, 2004.
(3) Abd-El-Aziz, A. S. *Macromol. Rapid Commun.* **2002**, *23*, 995−1031.
(4) Abd-El-Aziz, A. S.; Shipman, P. O.; Boden, B. N.; McNeil, W. S. *Prog. Polym. Sci.* **2010**, *35*, 714−836.
(5) Grubbs, R. B. *J. Polym. Sci., Part A: Polym. Chem.* **2005**, *43*, 4323−4336.
(6) Whittell, G. R.; Manners, I. *Adv. Mater.* **2007**, *19*, 3439−3468.
(7) Moad, G.; Solomon, D. H. *The Chemistry of Radical Polymerization*, 2nd ed.; Elsevier Science: Oxford, UK, 2006.
(8) *Handbook of RAFT Polymerization*; Barner-Kowollik, C., Ed.; Wiley-VCH: Weinheim, Germany, 2008.
(9) Matyjaszewski, K.; Tsarevsky, N. V. *Nat. Chem.* **2009**, *1*, 276−288.
(10) Kamigaito, M.; Ando, T.; Sawamoto, M. *Chem. Rev.* **2001**, *101*, 3689−3745.
(11) Kamigaito, M.; Ando, T.; Sawamoto, M. *Chem. Rec.* **2004**, *4*, 159−175.
(12) Ouchi, M.; Terashima, T.; Sawamoto, M. *Chem. Rev.* **2009**, *109*, 4963−5050.
(13) Kamigaito, M. *Polym. J.* **2011**, *43*, 105−120.
(14) Matyjaszewski, K.; Xia, J. *Chem. Rev.* **2001**, *101*, 2921−2990.
(15) Braunecker, W. A.; Matyjaszewski, K. *Prog. Polym. Sci.* **2007**, *32*, 93−146.
(16) Rosen, B. M.; Percec, V. *Chem. Rev.* **2009**, *109*, 5069−5119.
(17) Hawker, C. J.; Bosman, A. W.; Harth, E. *Chem. Rev.* **2001**, *101*, 3661−3688.
(18) Macomber, D. W.; Hart, W. P.; Rausch, M. D. *J. Am. Chem. Soc.* **1982**, *104*, 884−886.
(19) Branham, K. E.; Mays, J. W.; Gray, G. M.; Sanner, R. D.; Overturf, G. E., III; Cook, R. *Appl. Organomet. Chem.* **1997**, *11*, 213−221.
(20) Tomita, I.; Ueda, M. *J. Inorg. Organomet. Polym. Mater.* **2006**, *15*, 511−518.
(21) Pittman, C. U., Jr.; Hirao, A. *J. Polym. Sci., Polym. Chem. Ed.* **1978**, *16*, 1197−1209.
(22) Jinnai, H.; Spontak, R. J.; Nishi, T. *Macromolecules* **2010**, *43*, 1675−1688.
(23) Nishi, T.; Fujinami, S.; Nakajima, K.; Sugimori, H.; Hatta, M.; Weber, M.; Jinnai, H. *J. Phys. Conf. Ser.* **2009**, *184*, 012030.
(24) Gass, M. H.; Koziol, K. K. K.; Windle, A. H.; Midgley, P. A. *Nano Lett.* **2006**, *6*, 376−379.
(25) Jinnai, H.; Tsuchiya, T.; Motoki, S.; Kaneko, T.; Higuchi, T.; Takahara, A. *Microscopy* **2013**, *62*, 243−258.
(26) Krishnan, R.; Srinivasan, K. S. V. *Macromolecules* **2003**, *36*, 1769−1771.
(27) Krishnan, R.; Srinivasan, K. S. V. *Macromolecules* **2004**, *37*, 3614−3622.

(28) Cañamero, P. F.; de la Fuente, J. L.; Madruga, E. L.; Fernández-García, M. *Macromol. Chem. Phys.* **2004**, *205*, 2221−2228.
(29) Dayananda, K.; Dhamodharan, R. *J. Polym. Sci., Part A: Polym. Chem.* **2004**, *42*, 902−915.
(30) Li, G.; Zhu, X.; Zhu, J.; Cheng, Z.; Zhang, W. *Polymer* **2005**, *46*, 12716−12721.
(31) Asandei, A. D.; Saha, G. *Macromolecules* **2006**, *39*, 8999−9009.
(32) de la Fuente, J. L.; Cañamero, P. F.; Fernández-García, M. *J. Polym. Sci., Part A: Polym. Chem.* **2006**, *44*, 1807−1816.
(33) Tsarevsky, N. V.; Bencherif, S. A.; Matyjaszewski, K. *Macromolecules* **2007**, *40*, 4439−4445.
(34) París, R.; Mosquera, B.; de la Fuente, J. L. *Eur. Polym. J.* **2008**, *44*, 2920−2926.
(35) Haoli, D. J.; Roy, S.; Singha, N. K. *J. Polym. Sci., Part A: Polym. Chem.* **2009**, *47*, 6526−6533.
(36) Tsarevsky, N. V.; Jakubowski, W. *J. Polym. Sci., Part A: Polym. Chem.* **2011**, *49*, 918−925.
(37) Ouchi, M.; Terashima, T.; Sawamoto, M. *Acc. Chem. Res.* **2008**, *41*, 1120−1132.
(38) Kato, M.; Kamigaito, M.; Sawamoto, M.; Higashimura, T. *Macromolecules* **1995**, *28*, 1721−1723.
(39) Takahashi, H.; Ando, T.; Kamigaito, M.; Sawamoto, M. *Macromolecules* **1999**, *32*, 3820−3823.
(40) Ando, T.; Kamigaito, M.; Sawamoto, M. *Macromolecules* **2000**, *33*, 2819−2824.
(41) Hamasaki, S.; Kamigaito, M.; Sawamoto, M. *J. Polym. Sci., Part A: Polym. Chem.* **2002**, *40*, 617−623.
(42) Verkade, J. G. *Acc. Chem. Res.* **1993**, *26*, 483−489.
(43) Verkade, J. G. *Coord. Chem. Rev.* **1994**, *137*, 233−295.
(44) Menge, W. M. P. B.; Verkade, J. G. *Inrog. Chem.* **1991**, *30*, 4628−4631.
(45) Nugent, W. A.; Harlow, R. L. *J. Am. Chem. Soc.* **1994**, *116*, 6142−6148.
(46) Kim, Y.; Hong, E.; Lee, M. H.; Kim, J.; Han, Y.; Do, Y. *Organometallics* **1999**, *18*, 36−39.
(47) Kim, Y.; Do, Y. *Macromol. Rapid Commun.* **2000**, *21*, 1148−1155.
(48) Motokucho, S.; Takeuchi, D.; Sanda, F.; Endo, T. *Tetrahedron* **2001**, *57*, 7149−7152.
(49) Zaitsev, K. V.; Karlov, S. S.; Zabalov, M. V.; Churakov, A. V.; Zaitseva, G. S.; Lemenovskii, D. A. *Russ. Chem. Bull. Int. Ed.* **2005**, *54*, 2831−2840.
(50) Capel-Sanchez, M. C.; Blanco-Brieva, G.; Campos-Martin, J. M.; De Frutos, M. P.; WEn, A.; Rodriguez, J. A.; Fierro, J. L. G. *Langmuir* **2009**, *25*, 7148−7155.
(51) Watanabe, Y.; Ando, T.; Kamigaito, M.; Sawamoto, M. *Macromolecules* **2001**, *34*, 4370−4374.
(52) Mecerreyes, D.; Atthoff, B.; Boduch, K. A.; Trollsås, M.; Hedrick, J. L. *Macromolecules* **1999**, *32*, 5175−5182.
(53) Jeanguillaume, C.; Trebbia, P.; Colliex, C. *Ultramicroscopy* **1978**, *3*, 237−242.
(54) Egerton, R. F. *Electron Energy-loss Spectroscopy in the Transmission Electron Microscope*; Plenum Press: New York, 1996.
(55) Miura, Y.; Kaneko, T.; Satoh, K.; Kamigaito, M.; Jinnai, H.; Okamoto, Y. *Chem. Asian J.* **2007**, *2*, 662−672.
(56) Luther, P. K.; Lawrence, M. C.; Crowther, R. A. *Ultramicroscopy* **1988**, *24*, 7−18.
(57) Crowther, R. A.; DeRosier, D. J.; Klug, A. *Proc. R. Soc. London, A* **1970**, *317*, 319−340.